ELSEVIER

Inorganica Chimica Acta 229 (1995) 61–75

Inorganica Chimica Acta

Activation of dinuclear gold(I) ylide complexes by Lewis acids. Isomerization of *trans*-$[Au(CH_2)_2PPhMe]_2$, and the crystal structures of $[Au(CH_2)_2PPhMe]_2$, $[Au(CH_2)_2PPhMe]_2[SO_2]_2$, $[Au(CH_2)_2PPh_2]_2[SO_2]_2$ and $[Au(CH_2)_2PPhMe]_2[S_2CNEt_2]_2$ ☆

Dwight D. Heinrich, Richard J. Staples, John P. Fackler, Jr.*

Laboratory for Molecular Structure and Bonding and the Department of Chemistry, Texas A&M University, College Station, TX 77843, USA

Received 28 March 1994; revised 3 June 1994

Abstract

The compound $Au(CH_2)_2PPhMe]_2$ has been made in greater than 90% isomeric purity as the *trans* isomer. Isomerization occurs in solution leading to a mixture of the *cis* and *trans* isomers in a 47% to 53% ratio. Addition of strong protonic acids produces previously characterized monomeric Au(I) species. Weaker acids catalyze the isomerization of the dimer. When deutero-acids are used no deuterium incorporation into the ligands is observed. Lewis acids such as Me_3SnCl, $(Ph_3Au)NO_3$ and SO_2 also catalyze the isomerization. Crystal structures of $[Au(CH_2)_2PPhMe]_2$ and SO_2 adducts $[Au(CH_2)_2PPhMe]_2[SO_2]_2$ and $[Au(CH_2)_2PPh_2]_2[SO_2]_2$ are presented. A mechanism involving formation of a partial Au–Au bond and Au–C bond rupture, followed by formation of a chelating ylide ligand which can undergo the reverse processes using either ylide–methylene center is proposed for the acid catalyzed isomerization. Oxidation with tetraethyldithiuram disulfide results in the metal–metal bonded complex $[Au(CH_2)_2PPhMe]_2[S_2CNEt_2]_2$. For $[Au(CH_2)_2PPhMe]_2$, $P2_1$, $a=7.432(1)$, $b=13.826(2)$, $c=9.261(1)$ Å, $\beta=99.98(1)°$, $V=937.2(2)$ Å^3, $R=0.0494$, $R_w=0.0681$ for 2070 reflections with ($I<3\sigma(I)$) and 180 parameters. For $[Au(CH_2)_2PPhMe]_2[SO_2]_2$, $P2_1/c$, $a=9.478(3)$, $b=10.259(5)$, $c=24.583(6)$ Å, $\beta=99.77(2)°$, $V=2356(2)$ Å^3, $R=0.0540$, $R_w=0.0613$ for 1556 reflections with 158 parameters. For $[Au(CH_2)_2PPh_2]_2[SO_2]_2$, $C2/c$, $a=13.698(5)$, $b=12.630(4)$, $c=17.348(4)$ Å, $\beta=103.26(2)°$, $V=2927(2)$ Å^3, $R=0.0458$, $R_w=0.0620$ for 1973 reflections ($I>3\sigma(I)$) and 181 parameters. For $[Au(CH_2)_2PPhMe]_2[S_2CNEt_2]_2$, $P\bar{1}$, $a=10.423(3)$, $b=11.970(3)$, $c=7.522(2)$ Å, $\alpha=96.46(2)$, $\beta=91.06(2)$, $\gamma=73.06(2)°$, $V=893.4$ Å^3, $R=0.0231$, $R_w=0.0325$ for 2122 reflections ($I>4\sigma(I)$), 172 parameters.

Keywords: Crystal structures; Gold complexes; Ylide complexes; Lewis acid complexes; Dinuclear complexes

1. Introduction

In recent years much new knowledge has been gained regarding the chemistry of gold [1–3] including its role in medicine [2]. Our interest in gold has included the preparation and structural characterization of dinuclear gold ylide dimers, with the gold centers in the +1, +2 or +3 oxidation states. A major focus of this work has been on oxidative addition reactions of halide and alkylhalide molecules with the dinuclear gold(I) complexes to give dinuclear gold(II) complexes [4]. Although we have ventured into other aspects of gold chemistry, including trimeric compounds [5] and dimeric species [6] bridged by the ligand 1,1-dicyanoethylene-2,2-dithiolate (i-MNT), our interest in dinuclear gold ylide chemistry continues [7].

Much of our dinuclear gold ylide chemistry has dealt with the compound $[Au(CH_2)_2P(C_6H_5)_2]_2$ (**1**). It was discovered early in our work [7b] that the unsymmetrical Au(I) dimer $[Au(CH_2)_2P(C_6H_5)(CH_3)]_2$ (**2**) could be made in a pure *trans* configuration. Under the proper conditions this complex would isomerize to a mixture of both *cis* and *trans* isomers.

Jandik and Schmidbaur [8] also demonstrated isomerization by showing that if two different gold(I) ylide dimer complexes, each containing a different bridging

☆ This manuscript is dedicated to Professor F. Albert Cotton, a colleague, mentor and friend on the occasion of his 65th birthday and the recognition that 100 students (greater than 95% following after the senior author) have completed their Ph.D. studies under his guidance.

* Corresponding author.

SSDI 0020-1693(94)04227-M

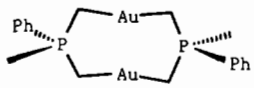

trans isomer

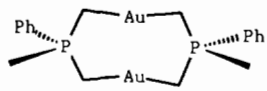

cis isomer

ligand, are mixed in CH_2Cl_2 a scrambling of the bridging ligands occurs leading to a equilibrium mixture of the three possible dimers.

Symmetrical ring cleavage of **1** by hydrogen halides has been reported [9]. The possibility was suggested that this reaction involves a dinuclear intermediate containing one bridging ylide ligand, one terminal ylide ligand and one terminal halide ligand. The possible relationship between ring cleavage processes and the isomerization of **2** has prompted us to take a close look at the conditions involved in the isomerization.

This paper reports a study of the isomerization of **2** in CD_2Cl_2, and describes how the addition of acid and base influence the isomerization process. The addition of the Lewis acid SO_2, for example, to the *trans* isomer of **2** catalyzes the isomerization, leading to the equilibrium mixture of *cis* and *trans* isomers. The crystal structure of **2** is described, as are the structures of the SO_2 adducts of **1** and **2**. A plausible mechanism for the isomerization of **2** involving the participation of Lewis acids is presented. The structure of the oxidative addition product of **2** with tetraethyldithiuram disulfide is also reported showing the formation of a discrete metal–metal bond. A preliminary communication of the structure of the SO_2 adduct of **1** has been published [10].

2. Experimental

2.1. Starting materials

Gold metal was purchased from Hauser&Miller, Co., St. Lewis, and converted to $Au(PPh_3)Cl$ using standard procedures [11]. SO_2 was purchased from Matheson and used as received. All phosphines were purchased from Strem Chemicals. BF_3-etherate and $SnMe_3Cl$ were purchased from Alfa Products. CH_2Cl_2, CF_3CO_2D and CD_3CO_2D were purchased from ICN Biomedicals. Ph_3MePBr and tetraethyldithiuram disulfide were purchased from Aldrich. KOH was purchased from Fisher. The $KOCH_3$ used here was a mixture of KOH and $KOCH_3$ prepared by dissolving 0.80 g of KOH in 30 ml of MeOH, then removing the solvent under vacuum with heating (50 °C). Ph_3PAuNO_3 was prepared from Ph_3PAuCl and $AgNO_3$ in CH_2Cl_2/MeOH, stirred overnight, filtered and crystallized using ether. The ylide $Ph_3(CH_2)P$ was prepared using established methods [4e]. PPN acetate, $PPN=[Ph_3P]_2N^+$, was graciously provided by Donald Darensbourg. All solvents used in syntheses were freshly distilled before use.

2.1.1. Preparation of $[Me_3PhP]I$

To a 500 ml Schlenk flask containing 150 ml THF were added 10.0 g (7.24×10^{-2} mol) Me_2PhP under a flow of argon. The flask was cooled to −20 °C using a dry ice-acetone bath. To this stirred solution was slowly added 5.4 ml (8.7×10^{-2} mol) of CH_3I (Aldrich). The solution was allowed to warm slowly to room temperature and stirred for 5 h, at which time the solution was pumped off. Yield 20.0 g, 99%.

2.1.2. Preparation of $[Me_2Ph_2P]I$

$[Me_2Ph_2P]I$ was prepared using a method identical to that of $[Me_3PhP]I$. A solution of 10.1 g (5.04×10^{-2} mol) of Me_2Ph_2P in 150 ml of THF was cooled to −20 °C. 4.0 ml of CH_3I (6.4×10^{-2} mol) were added and the mixture allowed to warm to room temperature and stir overnight. After removal of the solvent the yield was 14.2 g, 82.1%.

2.1.3. Preparation of $Li[(CH_2)_2PMePh]$

In a 200 ml Schlenk flask, equipped with a magnetic stir bar and septum and containing 50 ml of diethyl ether were placed 4.20 g (1.50×10^{-2} mol) of $[Me_2Ph_2P]I$. Under constant argon flow the septum was removed and 10 ml (1.5×10^{-2} mol) of 1.2 M CH_3Li in Et_2O (Alfa) were added. CH_4 was given off and the insoluble precipitate slowly disappeared leaving a yellow solution. A second 10 ml portion of CH_3Li was added. CH_4 was once more given off. After the gas evolution slowed, the septum was replaced and a one-way mercury bubbler attached. Stirring was continued for 7 h after which time the highly air sensitive (pyrophoric) solid was filtered under argon flow through a glass frit and washed with freshly distilled diethyl ether (300 ml) to remove LiI. A white solid was isolated (1.45 g, 9.2×10^{-3} mol, 61%). The appearance of a yellow discoloration indicated decomposition of the ylide anion to the ylide.

2.1.4. Preparation of $Li[(CH_2)_2PPh_2]$

This compound was made in a manner identical to that for $Li[(CH_2)_2PMePh]$. Using 3.05 g (8.91×10^{-3} mol) $[Me_2Ph_2P]I$ in 70 ml of THF and adding a total of 12.5 ml of 1.2 M CH_3Li (1.88×10^{-2} mol) in Et_2O yielded, after washing with 280 ml diethyl ether, 1.54 g (6.98×10^{-3} mol, 78.4%) of the $Li[(CH_2)_2PPh_2]$ ylide salt.

2.1.5. Preparation of $[Au(CH_2)_2PPh_2]_2$ (1)

Compound **1** was prepared in a method similar to that of **2** (see below). 1.10 g (5.0×10^{-3} mol) of $Li[(CH_2)_2PPh_2]$ were transferred to a Schlenk tube,

dissolved in 20 ml of toluene. 2.25 g (4.56×10^{-3} mol) of Ph_3PAuCl were added and the mixture stirred for 24 h. A white solid was filtered off and washed three times with MeOH (5 ml), THF (5 ml) and hexane (10 ml). After drying under vacuum the yield was 1.42 g (1.73×10^{-3} mol, 76%) of the desired product. M.p. = 242–245 °C. ^{1}H NMR ($CDCl_3$, ppm): 1.38 (doublet, J(P–H) = 12.0 Hz), 7.33 and 7.67 (m, Ph).

2.1.6. Preparation of $[Au(CH_2)_2PPhMe]_2$ (2)

0.500 g (3.16×10^{-3} mol) of slightly yellow $Li[(CH_2)_2PMeC_6H_5]$ was transferred to a Schlenk flask and dissolved in a mixture of 10 ml of toluene and 10 ml of THF. To the resulting yellow solution, 1.16 g (2.34×10^{-3} mol) of Ph_3PAuCl were added in one portion. The reaction mixture was stirred overnight after which time a white solid had precipitated. 10 ml of diethyl ether were added, the precipitate was filtered in air, and isolated as a slightly yellow solid. The solid was washed with spectroscopic grade methanol (10 ml), THF (4 ml), and finally with ether (10 ml). This washing procedure was repeated once again leaving a white solid, which, after drying on a vacuum line, yielded 0.610 g (8.76×10^{-4} mol, 74.8%) of the desired product. M.p. = 238–239 °C. ^{1}H NMR (CD_2Cl_2, ppm): $\delta(H_A)$ 0.898 (ABX multiplet, CH_2, *trans* isomer, $J(0)$ = 12.3, 12.9 Hz), 1.580 (doublet, CH_3, *trans* isomer, J(P–H) = 12.3 Hz); $\delta(H_B)$ 1.26 (ABX multiplet, *cis* isomer $J(0)$ = 12.3, 12.9 Hz). 1.807 (doublet, CH_3, *cis* isomer, J(P–H) = 12.3 Hz). Note: other methods for the preparation of **1** and **2** are available [4].

2.1.7. Preparation of $[Au(CH_2)_2PPhMe]_2[SO_2]_2$ (3)

In a typical preparation, 1.5×10^{-2} g (2.15×10^{-5} mol) of **2** were dissolved in 1.5 ml CH_2Cl_2 in a small vial. SO_2 was bubbled slowly through the colorless solution until a bright red color resulted. The solution was filtered into the bottom of a second vial containing 2 ml of heptane. The vial was capped and placed in the freezer for 48 h. When removed from the freezer, a mixture of red needles and clumps of small green plates had formed. Total yield was 1.01×10^{-2} g (1.23×10^{-5} mol, 57%). Upon warming and exposure to the atmosphere, the crystals quickly decomposed. ^{1}H NMR ($CDCl_3$, ppm) of red crystals: *trans* isomer 70%: 0.981 and 1.241 (ABX multiplet, CH_2, $J(0)$ = 12, 12.3 Hz), 1.601 (doublet, CH_3, J(P–H) = 12 Hz); *cis* isomer, 30%: 0.971 and 1.357 (ABX multiplet, CH_2, $J(0)$ = 12, 12.3 Hz), 1.804 (doublet, CH_3, J(P–H) = 12.0 Hz). Green crystals, 70% *cis*, 30% *trans*, NMR shifts identical to those found for the red crystals.

2.1.8. Preparation of $[Au(CH_2)_2PPh_2]_2[SO_2]_2$ (4)

A typical reaction involved dissolving 15 mg (1.83×10^{-5} mol) of **1** in 1.5 ml CH_2Cl_2, followed by a slow bubbling of SO_2 through the solution until a red color was achieved. The solution was filtered, layered with heptane and stored in the freezer for 2 days, yielding green–red dichroic crystals in 60% yield (10.4 mg, 1.10×10^{-5} mol). ^{1}H NMR ($CDCl_3$, ppm): 1.47 (doublet, CH_2, J(P–H) = 12.0 Hz), 7.33 and 7.77 (M, C_6H_5).

2.1.9. Preparation of $[Au(CH_2)_2PPhMe]_2[S_2CNEt_2]_2$ (5)

In a typical synthesis 0.040 g (5.80×10^{-5} mol) of **2** was dissolved in 5 ml of $CHCl_3$. To this solution 0.017 g (5.83×10^{-5} mol) of tetraethylthiuram disulfide was added. The solution slowly darkened to a deep red color. The solvent was removed and the product recrystallized from $CHCl_3$ and diethyl ether (0.0353 g, 61% yield; m.p. 172–175 °C). ^{1}H NMR ($CDCl_3$, ppm): 1.26 (t, CH_3–CH_2, J(H–H) = 6.9 Hz), 3.93 (q, –CH_2–CH_3, J(H–H) = 6.9 Hz), 1.73 and 1.93 (ABX multiplet, –CH_2–P, $J(0)$ = 11.8, 12.6 Hz), 1.92 (d, CH_3–P, J(P–H) = 12.6 Hz).

2.2. Kinetic studies

Data used for kinetic analysis of the isomerization of *trans*-**2** to an equilibrium mixture of the *cis* and *trans* isomers was collected on either a Varian XL-200 or a Varian XL-400 NMR Spectrometer.

2.2.1. Kinetic measurements

Rate data for the disappearance of *trans*-**2** were obtained by monitoring the changes observed in ^{1}H NMR spectra with time. In a typical experiment, 9.9 mg (1.42×10^{-5} mol) of **2** were placed in an NMR tube and dissolved in 1 ml CD_2Cl_2 (ICN Biomedicals) to give a 1.42×10^{-3} M solution. The sample was placed in the spectrometer and a constant temperature was maintained. A series of spectra was accumulated using a pre-acquisition delay (PAD) array set for the desired time intervals. The concentration of the *trans* isomer in each spectrum was determined by measuring the integral associated with the methyl doublet of the *trans* isomer and comparing it with the total integral region for the methyl doublets of both isomers. Plots of $-\ln C$ versus time for the disappearance of the *trans* isomer were linear until equilibrium was approached (about 3 half-lives). The slopes of these plots yielded K_{obs}.

The changes incurred by adding selected reagents (such as Me_3SnCl, SO_2, CD_3CO_2D, CF_3CO_2D and Ph_3PAuNO_3) were monitored by first obtaining a spectrum of a solution of **2** in CD_2Cl_2 or $CDCl_3$, then adding the desired compound, maintaining the temperature at 308 K for a period of 2–8 h, then measuring the amount of isomerization which had occurred by taking a second ^{1}H NMR spectrum and comparing the methyl peaks of the two isomers. The influence of the added base was determined using a series of THF

solutions containing **2** and the desired base, maintaining the solutions at 298 K for 3 days, removing solvent and measuring the extent of isomerization by ^{1}H NMR ($CDCl_3$). The extent of isomerization was compared with a blank of **2** prepared and run in an identical manner.

2.2.2. Deuterium incorporation studies

The possibility of deuterium incorporation was checked in three experiments utilizing ^{2}H NMR (Varian XL-200). **1**: 0.140 g (2.01×10^{-4} mol) of **2** in 5 ml $CHCl_3$, with 0.1 ml CD_3CO_2D, was stirred for 3 days. The solvent was removed and the isomerization was determined using 13.5 mg of the product via ^{1}H NMR. The product was found to be a mixture of the *cis* and *trans* isomers. The product (0.100 g) was dissolved in CH_2Cl_2 (5 ml) and a ^{2}H NMR was taken. No deuterium incorporation was observed. **2**: 0.110 g (1.58×10^{-4} mol) of **2** in 1.0 ml $CDCl_3$, 3.0 ml CH_2Cl_2 and 80 μl of CD_3CO_2D was monitored with ^{2}H NMR for 7 h. No incorporation occurred, although deuterium peaks for $CDCl_3$, CD_2Cl_2 and CD_3CO_2D were observed. **3**: To insure that deuterium incorporation would be observed if it had occurred, a 0.033 g sample of [ClAu(CH_2)PPhMe(CH_2D)] was prepared from **2** (70.2 mg, 1.01×10^{-4} mol) and DCl (0.2 ml, 38% in D_2O) [9] and was dissolved in CH_2Cl_2 (5 ml containing 0.1 ml of $CDCl_3$). ^{1}H NMR ($CDCl_3$, ppm): 1.654 (CH_2, $J(0)=12.4$ Hz, 2H) 1.993 (d, CH_3, $J(PH)\sim13$ Hz, 3H) 7.60 and 7.77 (m, Ph, 5H). ^{2}H NMR (CH_2Cl_2, ppm): 1.91 (broad, CH_2D). A 60 mg sample of **2** isomerized using 0.2 ml of CH_3CO_2D was dissolved in 5 ml CH_2Cl_2 and ^{2}H NMR under the same condition as above was obtained. No deuterium incorporation into the ylide ligand was observed.

2.3. X-ray data collection and reduction

X-ray crystallographic studies were performed using a Nicolet R3m/E diffractometer with graphite monochromated Mo Kα ($\lambda=0.71073$ Å) radiation. The SHELXTL data collection procedures (Versions 4.1 and 5.1) were used throughout. All calculations were performed on a Data General Eclipse S140 mini-computer. Data collection was performed at ambient temperature (25 °C).

Crystals of compound **2** were grown by slow diffusion of diethyl ether into a CH_2Cl_2 solution of **2**. The resulting crystals were large, clear, colorless blocks. The crystal used in data collection had the dimensions $0.20\times0.20\times0.35$ mm and was mounted on a glass fiber with epoxy. The initial orientation matrix and cell parameters were determined using 25 reflections taken from a rotation photo. Final lattice parameters and orientation matrix were determined using 24 reflections ($14<2\theta<30°$) obtained from a preliminary Wyckoff data collection. Compound **2** was found to belong to the monoclinic crystal system with $a=7.432(1)$, $b=13.826(2)$, $c=9.261(1)$ Å, $\beta=99.98(1)°$, $V=937.2(2)$ Å^3. A total of 2490 reflections was collected for $3<2\theta<55°$ with 3 check reflections collected every 97 reflections. No decay was observed in the check reflections. The data were corrected for intensity fluctuations in the standards, for absorption, and for Lorentz and polarization effects.

Crystals of **3** were grown by bubbling SO_2 through a $CHCl_3$ solution of **2**, layering with heptane and storing at −5 °C for 2 days. The crystals grown by this method were a mixture of tiny green plates and large red needles. Both crystal forms were observed to decompose when removed from solution, so a red needle was placed in mineral oil, cut to the dimensions, and reflections taken from a rotation photograph were used to obtain an initial orientation matrix. The red crystal was found to belong to the monoclinic crystal system. Final lattice parameters were determined using 15 reflections ($25<2\theta<28°$) with $a=9.478(3)$, $b=10.259(5)$, $c=24.583(6)$ Å, $\beta=99.77(2)°$, $V=2356(2)$ Å^3. Data collection was carried out using the $2\theta/\theta$ data collection method. Three low angle reflections were collected every 97 reflections as checks for decay. A decay of 27.3% was observed over the data collection period of 3657 total reflections ($3<2\theta<45°$). The data were corrected for intensity fluctuations, absorption, and for Lorentz and polarization effects.

Crystals of **4** were obtained by bubbling SO_2 through a CH_2Cl_2 solution of **1**, layering this solution with heptane and storing at −5 °C for 2 days. The crystals were green in color when removed from the freezer, but became red upon warming to room temperature. A large crystal of dimensions $0.50\times0.50\times0.60$ mm was cut, mounted at the top of a capillary tube and covered with epoxy. Initially, 25 reflections obtained from a rotation photo were used to determine the orientation matrix and preliminary cell parameters. A total of 23 reflections ($28<2\theta<34.5°$) was used to obtain the final cell parameters and orientation matrix. A monoclinic crystal system was indicated from the cell parameters of $a=13.698(5)$, $b=12.630(4)$, $c=17.348(4)$ Å, $\beta=103.26(2)°$, $V=2927(2)$ Å^3. The monoclinic system and axial lengths were confirmed by axial photographs. C centering for the crystal was confirmed by collecting 990 reflections without centering restrictions and noting the *hkl*: $h+k=2n$ systematic absences. The rest of the data were collected with C centering restriction. A total of 3417 reflections was collected with three low angle standard reflections collected every 97 reflections. A decay in the standard reflections of 32% was observed over the course of data collection. Corrections for decay, absorption, and Lorentz and polarization effects were made.

Crystals of **5** were grown from chloroform by slow diffusion of diethyl ether. Twelve reflections obtained from a rotation photograph were used in the initial cell parameters and orientation matrix determination. Final lattice parameters were determined using 25 reflections ($30<2\theta<35°$) giving $a=10.423(3)$, $b=11.970(3)$, $c=7.522(2)$ Å, $\alpha=96.46(2)$, $\beta=91.06(2)$, $\gamma=73.06(2)°$ and $V=892.0(4)$ Å^3 [1]. The axial lengths were confirmed by axial photographs. A total of 2587 reflections was collected with three low angle standard reflections collected every 97 reflections. A decay in the standard reflections of less than 1% was observed over the course of data collection. Corrections for decay, absorption, and Lorentz and polarization effects were made.

[1] An alternative synthesis involves the reaction of the Au^{II} dichloride or dibromide dimer with sodium diethyldithiocarbamate. In addition, a second crystal of **5** has been isolated by slow evaporation of a $CHCl_3$ solution. Its space group was determined to be $P2_1/c$; $a=12.213(4)$, $b=11.503(4)$, $c=15.67(4)$ Å, $\beta=102.2(3)°$, $V=1725(1)$ Å^3.

A complete list of data collection and solution parameters for **2**, **3**, **4** and **5** can be found in Table 1.

2.4. Structure solution and refinement

The structures of **2**, **3** and **4** were solved using standard heavy atom methods. The heavy atom positions in **2** were found using direct methods (SOLV, a program adapted from MULTAN-78). The heavy atom positions of **3** and **4** were found from sharpened Patterson maps. All other non-hydrogen atom positions in **2**, **3** and **4** were determined from successive cycles of least-squares refinements followed by generation of difference Fourier maps. Empirical absorption corrections were applied to all three structures based on azimuthal scans (for **2**, nine reflections $8<2\theta<23°$; for **3**, ten reflections $4<\theta<15°$; for **4**, ten reflections $8<2\theta<30°$).

The refinement of compound **2** initially was carried out in the space group $P2_1/m$, but failed to refine successfully (lowest $R=0.2598$ with two gold and two phosphorous atoms). Refinement in the non-centrosymmetric space group $P2_1$ was successful. All non-

Table 1
Crystallographic data for **2**, **3**, **4** and **5**

	2	**3**	**4**	**5**
Formula	$C_{18}H_{24}Au_2P_2$	$C_{18}H_{24}Au_2P_2S_2O_4$	$C_{28}H_{28}Au_2P_2S_2O_4$	$C_{28}H_{44}N_2P_2S_4Au_2$
Formula weight (a.m.u.)	696.27	824.39	948.54	992.8
Space group	$P2_1$ (No. 4)	$P2_1/c$ (No. 14)	$C2/c$ (No. 15)	$P\bar{1}$ (No. 2)
a (Å)	7.432(1)	9.478(3)	13.698(5)	10.423(3)
b (Å)	13.826(2)	10.259(5)	12.630(4)	11.970(3)
c (Å)	9.261(2)	24.583(6)	17.348(4)	7.522(2)
α (°)	90.000	90.000	90.000	96.46(2)
β (°)	99.98(1)	99.77(2)	103.26(2)	91.06(2)
γ (°)	90.000	90.000	90.000	73.06(2)
Volume (Å^3)	937.2(2)	2356(2)	2927(2)	892.0(4)
Z	2	4	8	1
D_{calc} (g cm^{-3})	2.47	2.32	2.16	1.845
Crystal size (mm)	0.2×0.2×0.4	0.2×0.1×0.8	0.5×0.5×0.6	0.1×0.2×0.2
$F(000)$ (e)	640	1536	1792	478
μ (Mo Kα) (cm^{-1})	157.7	127.5	102.9	8.521
Radiation graphite monochromated (Å)	Mo Kα, 0.71073	Mo Kα, 0.71073	Mo Kα, 0.71073	Mo Kα, 0.71073
Orientation reflections, 2θ: no., range	25, 14–30	15, 25–29	23, 28–35	25, 30–35
Temperature (K)	293	293	293	295
Scan method	ω	$\theta/2\theta$	ω	$\theta/2\theta$
Data collection range, 2θ (°)	3–55	3–45	0–50	3–45
Total reflections measured	2490	3657	3417	2587
No. unique reflections	2245	3090	3303	2349
No. with $F_o^2>3\sigma(F_o^2)$	2070	1556	1973	2122
No. parameters refined	180	158	181	172
Transmission factor: max., min.	0.532, 0.227	0.995, 0.355	1.000, 0.390	0.964, 0.610
R [a], R_w [b]	0.0494, 0.0681	0.0540, 0.0613	0.0458, 0.0620	0.0231, 0.0325
S, GOF [c]	0.747	1.354	1.225	1.30
Largest shift/e.s.d., final cycle	0.005	0.001	0.011	0.086
Largest peak (e Å^{-3})	1.74	1.31	3.14	0.64
g	0.00685	0.00077	0.00173	0.0004

[a] $R=\Sigma||F_o|-|F_c||/\Sigma|F_o|$.
[b] $R_w=[\Sigma\sqrt{w}(|F_o|-|F_c|)]/\Sigma\sqrt{w}|F_o|$; $w^1=[\sigma^2(|F|)+g|F_o|^2]$.
[c] Goodness-of-fit $=[\Sigma w(|F_o|-|F_c|)^2/(N_o-N_p)]^{1/2}$.

hydrogen atoms were refined anisotropically. An Au atom, Au(1), was fixed with its y coordinate at 1/4. Phenyl rings were refined as rigid bodies (C–C distances = 1.395 Å). Hydrogen atoms were placed at calculated positions (C–H = 0.960 Å) on all phenyl, methyl and methylene carbon atoms during the final cycles of refinement. Thermal parameters for the hydrogen atoms were fixed at 1.2 times the thermal parameter of the atom to which they were attached. Refinement in this manner lead to final R values of $R = 0.0494$, $R_w = 0.0681$ and a goodness-of-fit (*GOF*) indicator of 0.747. A check to establish the correct enantiomer was performed by transformation to and refinement of the second enantiomer ($R = 0.0506$, $R_w = 0.0712$). The initial enantiomer was used for the final structure of **2**. The final R values were determined using 180 parameters and 2070 reflections with $I > 3\sigma(I)$. Atomic positional parameters for **2** are given in Table 2; significant bond distances and angles are given in Table 3.

The solution of the structure of compound **3** was carried out in the space group $P2_1/c$. A Patterson map yielded the location of the first heavy atom position. A second gold atom position was found from the first difference Fourier map. The positions of the other non-hydrogen atoms were found subsequently, including a complex disorder between two methyl and two methylene positions. Refinement of this disorder and the large thermal ellipsoid associated with the second gold atom suggested that refinement of the second gold center should be done at two disordered metal positions. Structure occupancy factors (SOF) for the methyl, methylene and gold disorders were refined using free variables (methyl C(3a) and methylene C(6a) were tied to a free variable with methyl C(3b) and methylene C(6b) set to 1 minus the SOF of C(3a) and C(6a), respectively, while the SOF of Au(3) was set to 1 minus the SOF of Au(2), which was tied to a second free

Table 2
Atomic coordinates ($\times 10^4$) and isotropic thermal parameters ($Å^2 \times 10^3$)[a] for $[Au(CH_2)_2P(C_6H_5)(CH_3)]_2$

Atom	x	y	z	U_{iso}[b]
Au(1)	8243(1)	7500	9495(1)	44(1)
Au(2)	5227(1)	8955(1)	8751(1)	42(1)
P(1)	8613(7)	9094(4)	7081(5)	42(1)
P(2)	4883(6)	7449(4)	11234(4)	42(1)
C(1)	9185(30)	7923(22)	7598(25)	60(8)
C(2)	6266(35)	9356(19)	6853(21)	60(7)
C(3)	7318(26)	7246(17)	11463(19)	47(6)
C(4)	4326(30)	8667(14)	10738(25)	50(6)
C(11)	8269(13)	9477(12)	4098(13)	55(7)
C(12)	8899(13)	9726(12)	2814(13)	60(8)
C(13)	10741(13)	9941(12)	2859(13)	62(8)
C(14)	11954(13)	9906(12)	4188(13)	68(9)
C(15)	11324(13)	9657(12)	5473(13)	68(9)
C(16)	9481(13)	9443(12)	5428(13)	45(6)
C(21)	2242(14)	7301(13)	13006(11)	59(8)
C(22)	1616(14)	7162(13)	14326(11)	74(10)
C(23)	2844(14)	6926(13)	15593(11)	52(6)
C(24)	4700(14)	6828(13)	15539(11)	66(9)
C(25)	5326(14)	6967(13)	14219(11)	50(6)
C(26)	4098(14)	7204(13)	12952(11)	41(5)
C(30)	9696(29)	9892(15)	8467(20)	46(6)
C(40)	3756(43)	6601(18)	9990(28)	73(10)

[a] E.s.d.s in the least significant digits are given in parentheses.
[b] Equivalent isotropic U is defined as 1/3 of the trace of the U_{ij} tensor.

Table 3
Significant bond lengths (Å) and angles (°)[a] for $[Au(CH_2)_2P(C_6H_5)(CH_3)]_2$

Au(1)–Au(2)	3.002(1)	Au(1)–C(1)	2.084(25)
Au(1)–C(3)	2.086(19)	Au(2)–C(2)	2.113(23)
Au(2)–C(4)	2.102(24)	P(1)–C(1)	1.721(30)
P(1)–C(2)	1.758(26)	P(1)–C(16)	1.826(14)
P(1)–C(30)	1.777(19)	P(2)–C(3)	1.807(20)
P(2)–C(4)	1.775(20)	P(2)–C(26)	1.820(12)
P(2)–C(40)	1.751(26)		
Au(2)–Au(1)–C(1)	88.0(7)	Au(2)–Au(1)–C(3)	88.1(6)
C(1)–Au(1)–C(3)	173.3(10)	Au(1)–Au(2)–C(2)	90.0(7)
Au(1)–Au(2)–C(4)	90.6(6)	C(2)–Au(2)–C(4)	174.7(8)
C(1)–P(1)–C(2)	114.8(12)	C(1)–P(1)–C(16)	112.1(10)
C(2)–P(1)–C(16)	109.4(8)	C(1)–P(1)–C(30)	108.9(10)
C(2)–P(1)–C(30)	105.9(11)	C(16)–P(1)–C(30)	105.0(9)
C(3)–P(2)–C(4)	111.2(11)	C(3)–P(2)–C(26)	109.5(7)
C(4)–P(2)–C(26)	107.9(10)	C(3)–P(2)–C(40)	109.2(13)
C(4)–P(2)–C(40)	113.6(11)	C(26)–P(2)–C(40)	105.1(11)
Au(1)–C(1)–P(1)	113.3(14)	Au(2)–C(2)–P(1)	110.1(10)
Au(1)–C(3)–P(2)	110.2(9)	Au(2)–C(4)–P(2)	108.1(11)
P(1)–C(16)–C(11)	118.7(3)	P(1)–C(16)–C(15)	121.3(3)
P(2)–C(26)–C(21)	118.8(4)	P(2)–C(26)–C(25)	121.1(3)

[a] E.s.d.s in the least significant digits are given in parentheses.

variable). The SOF of Au(2), C(3a) and C(6a) were refined at 60% occupancy (61.31% for Au and 59.7% for the C atoms). Only one of the two sulfur atoms connected to Au(2) and Au(3) could be found suggesting that 25% of the SO_2 had been lost. Other causes of this disorder are discussed vide infra. Only the gold, phosphorus and oxygen positions were refined anisotropically. No hydrogen atoms were used during refinement. Phenyl rings were fixed as rigid groups (C–C = 1.395 Å). The final refinement using 158 parameters and 1556 reflections ($I > 3\sigma(I)$) gave R values of $R = 0.0540$, $R_w = 0.0613$ and a goodness-of-fit (*GOF*) indicator of 1.354. Atomic positional parameters for **3** are given in Table 4. Significant bond distances and angles are given in Table 5 for the higher occupancy (model a) structure.

The structure of compound **4** was solved in the space group *C2/c*. All non-hydrogen atoms were refined anisotropically. Hydrogen atoms were placed at calculated positions for phenyl and methylene carbon atoms (C–H distance = 0.960 Å). A disorder in one oxygen of the

Table 4
Atomic coordinates ($\times 10^4$) and isotropic thermal parameters ($Å^2 \times 10^3$) [a] for $[Au(CH_2)_2P(C_6H_5)(CH_3)]_2[SO_2]_2$

Atom	x	y	z	U_{iso} [b]
Au(1)	−1062(1)	7401(1)	3306(1)	46(1)*
Au(2)	1154(11)	5727(15)	3016(2)	63(2)*
Au(3)	1530(7)	6439(19)	2996(2)	50(3)*
P(1)	−1420(7)	6271(7)	2087(3)	48(3)*
P(2)	1474(7)	6424(8)	4257(3)	64(3)*
S(1)	−2993(7)	9041(7)	3568(3)	64(3)*
O(1)	−2197(21)	9757(19)	4021(9)	81(9)*
O(2)	−4051(22)	8187(23)	3702(11)	116(12)*
S(2)	4035(8)	6417(9)	2747(4)	79(4)*
O(3)	3847(23)	6957(25)	2201(11)	112(12)*
O(4)	4580(23)	5123(27)	2764(12)	136(14)*
C(4)	−2121(30)	4751(29)	2322(13)	77(9)
C(5)	−167(26)	7268(25)	4145(12)	63(8)
C(1)	511(25)	6217(24)	2179(11)	55(7)
C(2)	−2031(24)	7636(24)	2456(10)	51(7)
C(3a)	1816(43)	5250(42)	3870(19)	54(16)
C(3b)	2698(64)	6382(62)	3818(28)	60(23)
C(6a)	2882(50)	7863(46)	4103(22)	76(19)
C(6b)	620(65)	4600(65)	4076(29)	62(24)
C(31)	−1359(14)	6106(18)	949(8)	70(9)
C(32)	−1977(14)	6137(18)	393(8)	83(10)
C(33)	−3433(14)	6410(18)	240(8)	99(11)
C(34)	−4269(14)	6652(18)	645(8)	115(13)
C(35)	−3651(14)	6620(18)	1201(8)	90(10)
C(36)	−2196(14)	6347(18)	1354(8)	42(6)
C(91)	1861(19)	7140(15)	5363(9)	96(11)
C(92)	2388(19)	6979(15)	5924(9)	93(11)
C(93)	3197(19)	5880(15)	6107(9)	76(9)
C(94)	3480(19)	4941(15)	5729(9)	80(10)
C(95)	2954(19)	5102(15)	5168(9)	64(8)
C(96)	2144(19)	6201(15)	4985(9)	49(7)

[a] E.s.d.s in the least significant digits are given in parentheses.
[b] For values with asterisks, the equivalent isotropic U is defined as 1/3 of the trace of the U_{ij} tensor.

Table 5
Bond lengths (Å) and angles (°) [a] for $[Au(CH_2)_2P(C_6H_5)(CH_3)]_2[SO_2]_2$

Au(1)–Au(2)	2.894(12)	Au(1)–Au(3)	2.868(10)
Au(1)–S(1)	2.645(8)	Au(1)–C(5)	2.097(27)
Au(1)–C(2)	2.148(24)	Au(2)–Au(3)	0.818(23)
Au(2)–C(1)	2.106(26)	Au(2)–C(3a)	2.142(44)
Au(2)–C(3b)	2.345(61)	Au(3)–S(2)	2.551(11)
Au(3)–C(1)	2.089(25)	Au(3)–C(3b)	2.133(63)
P(1)–C(4)	1.827(31)	P(1)–C(1)	1.806(24)
P(1)–C(2)	1.816(26)	P(1)–C(36)	1.829(20)
P(2)–C(5)	1.761(26)	P(2)–C(3a)	1.601(46)
P(2)–C(3b)	1.712(70)	P(2)–C(96)	1.810(22)
S(1)–O(1)	1.436(20)	S(1)–O(2)	1.411(25)
S(2)–O(3)	1.433(28)	S(2)–O(4)	1.422(28)
C(3a)–C(3b)	1.449(76)	C(3a)–C(6b)	1.476(81)
C(3b)–C(6a)	1.669(81)		

Au(3)–Au(1)–S(1)	160.6(4)
Au(3)–Au(1)–C(5)	91.0(7)
Au(2)–Au(1)–C(2)	92.0(7)
S(1)–Au(1)–C(2)	88.1(7)
Au(2)–Au(1)–S(1)	176.9(3)
Au(2)–Au(1)–C(5)	90.8(7)
S(1)–Au(1)–C(5)	89.0(7)
Au(3)–Au(1)–C(2)	91.4(7)
C(5)–Au(1)–C(2)	176.9(10)
Au(1)–Au(2)–C(1)	89.8(8)
Au(3)–Au(2)–C(1)	77.6(9)
Au(3)–Au(2)–C(3a)	101.8(13)
Au(1)–Au(2)–C(3b)	89.9(16)
C(1)–Au(2)–C(3b)	142.1(19)
Au(1)–Au(3)–Au(2)	83.7(10)
Au(2)–Au(3)–S(2)	116.1(14)
Au(2)–Au(3)–C(1)	80.0(9)
Au(1)–Au(3)–C(3b)	95.1(18)
S(2)–Au(3)–C(3b)	82.7(18)
C(4)–P(1)–C(1)	110.5(12)
C(1)–P(1)–C(2)	111.3(11)
C(1)–P(1)–C(36)	110.7(11)
C(5)–P(2)–C(3a)	122.6(17)
C(3a)–P(2)–C(3b)	51.7(26)
C(3a)–P(2)–C(96)	114.9(16)
Au(1)–S(1)–O(1)	102.7(9)
O(1)–S(1)–O(2)	115.9(15)
Au(3)–S(2)–O(4)	110.4(12)
Au(1)–C(5)–P(2)	112.6(15)
Au(2)–C(1)–P(1)	104.4(13)
Au(1)–C(2)–P(1)	106.2(11)
Au(2)–C(3a)–C(3b)	79.0(32)
Au(2)–C(3a)–C(6b)	108.9(33)
C(3b)–C(3a)–C(6b)	151.6(51)
Au(2)–C(3b)–P(2)	98.3(26)
Au(2)–C(3b)–C(3a)	63.7(27)
P(2)–C(3b)–C(3a)	60.2(31)
Au(3)–C(3b)–C(6a)	111.9(36)
C(3a)–C(3b)–C(6a)	135.5(55)
Au(1)–Au(2)–C(3a)	89.9(12)
C(1)–Au(2)–C(3a)	179.4(11)
Au(3)–Au(2)–C(3b)	65.1(17)
C(3a)–Au(2)–C(3b)	37.3(20)
Au(1)–Au(3)–S(2)	160.2(8)
Au(1)–Au(3)–C(1)	90.9(7)
S(2)–Au(3)–C(1)	93.7(8)
Au(2)–Au(3)–C(3b)	94.6(19)
C(1)–Au(3)–C(3b)	171.4(21)

(*continued*)

Table 5 (*continued*)

C(4)–P(1)–C(2)	109.7(14)
C(4)–P(1)–C(36)	103.9(11)
C(2)–P(1)–C(36)	110.5(10)
C(5)–P(2)–C(3b)	126.1(23)
C(5)–P(2)–C(96)	111.6(12)
C(3b)–P(2)–C(96)	117.3(21)
Au(1)–S(1)–O(2)	102.1(10)
Au(3)–S(2)–O(3)	104.4(10)
O(3)–S(2)–O(4)	112.0(17)
Au(2)–C(1)–Au(3)	22.5(7)
Au(3)–C(1)–P(1)	114.2(14)
Au(2)–C(3a)–P(2)	110.8(22)
P(2)–C(3a)–C(3b)	68.1(33)
P(2)–C(3a)–C(6b)	83.8(35)
Au(2)–C(3b)–Au(3)	20.3(8)
Au(3)–C(3b)–P(2)	107.3(29)
Au(3)–C(3b)–C(3a)	83.7(32)
Au(2)–C(3b)–C(6a)	128.3(36)
P(2)–C(3b)–C(6a)	75.4(34)
P(1)–C(36)–C(31)	120.8(5)
P(1)–C(36)–C(35)	119.1(5)
P(2)–C(96)–C(95)	120.2(6)
P(2)–C(96)–C(91)	119.8(6)

[a] E.s.d.s in the least significant digits are given in parentheses.

Table 6
Atomic coordinates ($\times 10^4$) and isotropic thermal parameters ($Å^2 \times 10^3$) [a] for $[Au(CH_2)_2P(C_6H_5)_2]_2[SO_2]_2$

Atom	*x*	*y*	*z*	U_{iso} [b]
Au	3380(1)	8105(1)	5287(1)	42(1)
S(1)	4877(3)	9246(4)	6012(4)	117(3)
O(1)	5681(9)	8904(11)	5703(8)	125(6)
O(2a)	4981(17)	9064(33)	6837(13)	164(17)
O(2b)	4595(26)	10091(20)	6211(26)	191(19)
P(1)	1501(2)	9316(2)	4209(2)	40(1)
C(1)	2561(9)	9518(8)	5018(7)	49(4)
C(2)	766(9)	8250(8)	4437(8)	51(4)
C(11)	−166(11)	10520(11)	3522(9)	73(6)
C(12)	−700(12)	11463(14)	3365(10)	93(7)
C(13)	−276(12)	12389(11)	3635(10)	76(6)
C(14)	650(10)	12418(10)	4102(9)	76(6)
C(15)	1177(10)	11507(10)	4281(9)	62(5)
C(16)	782(8)	10523(8)	3990(6)	42(4)
C(21)	1608(12)	8126(9)	2850(8)	63(5)
C(22)	1898(13)	7954(11)	2171(8)	77(6)
C(23)	2592(14)	8729(15)	1957(9)	95(8)
C(24)	2875(12)	9600(13)	2399(9)	80(7)
C(25)	2561(9)	9746(10)	3071(8)	61(5)
C(26)	1916(8)	9060(9)	3317(6)	46(4)

[a] E.s.d.s in the least significant digits are given in parentheses.
[b] Equivalent isotropic *U* is defined as 1/3 of the trace of the U_{ij} tensor.

SO_2 ligand was refined with the SOF of each disordered position fixed at 50% occupancy. Final refinement using 181 parameters and 1974 reflections ($I > 3\sigma(I)$) gave *R* values of $R = 0.0458$, $R_w = 0.0620$ and $GOF = 1.225$. Atomic positional parameters for **4** are found in Table 6, with bond lengths and angles in Table 7.

The structure of compound **5** was solved in the space group $P\bar{1}$. Hydrogen atoms were placed at calculated positions for phenyl and methylene carbon atoms (C–H distance = 0.960 Å). All non-hydrogen atoms were refined anisotropically. Final convergence of 172 parameters gave *R* values of $R = 0.0231$ and $R_w = 0.0325$ using a weighting scheme and 2122 reflections with $I > 4\sigma(I)$. Atomic positional parameters for **4** are found in Table 8, with bond lengths and angles in Table 9.

3. Results

The rate of isomerization of **2**, Fig. 1, was monitored by following the changes in the ^1H NMR spectra with time, Fig. 2. The NMR spectra indicate that the isomerization of **2** proceeds from an approximately 9:1 mixture to a 1:1 mixture of the *trans* and *cis* isomers. No Au^{II} or Au^{III} side products are observed over the period of isomerization, although **2** in CH_2Cl_2 is known to produce both Au^{II} and Au^{III} products under more vigorous conditions [11]. The concentration of the *trans* isomer was determined in each spectrum from the ratio of the areas for the methyl doublet assigned to the individual isomers. Plots of $-\ln C$ versus time were linear, Fig. 3, for both the disappearance of the *trans* isomer and the appearance of the *cis* isomer. Values for k_{obs} were reproducible within the error of the experiments (Table 10).

The rate of the isomerization was substantially increased by the addition of acetic acid or SO_2, Fig. 3. The addition of stronger protonic acids (CF_3CO_2H, HCl, HBr) in two equivalent amounts of greater resulted in the rupture of the dimer ring and produced two monomeric Au^I units.

The addition of one equivalent of CF_3CO_2H to a solution of *trans*-**2** resulted in the rapid (1 h) isomerization of **2** to an equilibrium mixture of the *cis* and *trans* isomers, but also caused the rupture of half the dimers into monomers. When CH_3CO_2H was added to **2** the rate of isomerization was enhanced without the degradation of the dimers. The use of CD_3CO_2D to isomerize the *trans*-**2** did not show detectable deuterium incorporation into the ylide ligands in the ^2H NMR experiments performed. Deuterium incorporation was observed when CF_3CO_2D was used to rupture **2** into monomeric units under identical conditions.

The addition of Lewis acids (BF_3, $SnMe_3Cl$, SO_2) gave mixed success in catalyzing the isomerization of *trans*-**2**. The stronger Lewis acids produced drastic color changes in the $CHCl_3$ solutions of *trans*-**2**, and deposited brown or green insoluble precipitates which were uncharacterizable. The Lewis acids SO_2 and Me_3SnCl caused color changes from the colorless CH_2Cl_2 solution of **2** to orange and green, respectively. Isomerization of **2** was enhanced by these Lewis acids (Fig. 3) without

Table 7
Bond lengths (Å) and angles (°) [a] for $[Au(CH_2)_2P(C_6H_5)_2]_2[SO_2]_2$

Au–S(1)	2.587(5)	Au–C(1)	2.103(11)
Au–Aua	2.835(1)	Au–C(2a)	2.067(10)
S(1)–O(1)	1.398(15)	S(1)–O(2a)	1.427(25)
S(1)–O(2b)	1.211(31)	P(1)–C(1)	1.794(10)
P(1)–C(2)	1.778(12)	P(1)–C(16)	1.808(11)
P(1)–C(26)	1.799(12)	C(2)–Aua	2.067(10)
C(11)–C(12)	1.393(22)	C(11)–C(16)	1.367(16)
C(12)–C(13)	1.342(22)	C(13)–C(14)	1.340(20)
C(14)–C(15)	1.356(18)	C(15)–C(16)	1.403(16)
C(21)–C(22)	1.346(22)	C(21)–C(26)	1.440(16)
C(22)–C(23)	1.469(26)	C(23)–C(24)	1.348(24)
C(24)–C(25)	1.346(23)	C(25)–C(26)	1.372(18)
S(1)–Au–C(1)	87.6(3)	S(1)–Au–Aua	170.8(2)
C(1)–Au–Aua	90.7(3)	S(1)–Au–C(2a)	90.3(3)
C(1)–Au–C(2a)	177.8(4)	Aua–Au–C(2a)	91.4(3)
Au–S(1)–O(1)	104.2(6)	Au–S(1)–O(2a)	106.7(13)
O(1)–S(1)–O(2a)	115.4(13)	Au–S(1)–O(2b)	111.2(16)
O(1)–S(1)–O(2b)	135.3(20)	O(2a)–S(1)–O(2b)	79.7(26)
C(1)–P(1)–C(2)	109.3(5)	C(1)–P(1)–C(16)	110.4(5)
C(2)–P(1)–C(16)	112.2(5)	C(1)–P(1)–C(26)	110.1(5)
C(2)–P(1)–C(26)	111.2(6)	C(16)–P(1)–C(26)	103.5(5)
Au–C(1)–P(1)	110.4(5)	P(1)–C(2)–Aua	111.1(6)
C(12)–C(11)–C(16)	119.9(12)	C(11)–C(12)–C(13)	120.8(14)
C(12)–C(13)–C(14)	120.7(14)	C(13)–C(14)–C(15)	119.7(12)
C(14)–C(15)–C(16)	121.9(11)	P(1)–C(16)–C(11)	121.3(9)
P(1)–C(16)–C(15)	121.7(8)	C(11)–C(16)–C(15)	116.9(11)
C(22)–C(21)–C(26)	121.3(13)	C(21)–C(22)–C(23)	116.8(13)
C(22)–C(23)–C(24)	121.2(16)	C(23)–C(24)–C(25)	120.0(16)
C(24)–C(25)–C(26)	122.6(13)	P(1)–C(26)–C(21)	121.6(10)
P(1)–C(26)–C(25)	120.5(9)	C(21)–C(26)–C(25)	118.0(12)

[a] E.s.d.s in the least significant digits are given in parentheses.

producing any immediately observable side products. Crystals of an SO_2 adduct of **2** were grown, however, from a solution of **2** in $CHCl_3$ or CH_2Cl_2 layered with heptane and stored in the freezer for 1–2 days.

The observed rate enhancement of the isomerization of **2** by acids prompted a study of the effect of base addition. THF solutions of **2** were prepared and kept at a constant temperature (25 °C). The bases, KOMe/KOH mixture, and triphenylphosphine methylide were added to two of the solutions. After 24 h a blank showed complete isomerization, while the solutions containing the added bases showed substantial suppression of isomerization, Fig. 4.

An increase in the rate of isomerization of **2** was observed by NMR when one equivalent of Ph_3PAuNO_3 was added to a CD_2Cl_2 solution of *trans*-**2**. After 2 h in solution, however, the ^1H NMR indicated that about half of the original Au^I dimer had been converted to an Au^{II} product, leaving the remainder of the Au^I as a mixture of the *cis* and *trans* isomers. The addition of PPN acetate and triphenylmethyl phosphine bromide had no effect on the rate of isomerization of **2**.

The oxidation of **2** with tetraethyldithiuram disulfide produces the Au^{II}–Au^{II} metal–metal bonded complex $[Au(CH_2)_2PPhMe]_2[S_2CNEt_2]_2$ (**5**). The formation of a formal Au–Au bond can be seen from the Au–Au distance, 2.647(1) Å. The complex crystallizes in the *trans* geometry.

3.1. Crystal structures

The structure of **2**, Fig. 1, was solved in the non-centrosymmetric space group $P2_1$. Although the eight-membered dimer ring is nearly centrosymmetric, the orientation of the phenyl rings disrupt the center of symmetry, resulting in the necessary solution in the lower symmetry space group. The Au–Au distance is 3.003(1) Å, a non-bonding distance 0.036 Å longer than the Au–Au distance found [4a] in **1**. The Au–C distances which average 2.099(2) Å are typical of gold–ylide systems. The phosphorus–methylene distances range from 1.77(3) to 1.83(2) Å. This type of variation is often seen in gold ylide dimers. The P–CH_3 distances are very similar to each other and average 1.76(2) Å. The phosphorus–phenyl distances are also similar to each other, but are considerably longer with an average distance of 1.82(2) Å. As a whole the structure of **2** is very similar [4a] to **1**, and also to the dimethyl dimer reported [13] by Schmidbaur and Franke.

Table 8
Atomic coordinates ($\times 10^4$) and equivalent isotropic displacement parameters ($Å^2 \times 10^3$) [a] for $[Au_2(CH_2PPh(Me)CH_2)_2(S_2CN(Et)_2)_2]$

Atom	x	y	z	U_{eq} [b]
Au	523(1)	4602(1)	1504(1)	41(1)
P	1459(2)	6744(1)	423(2)	47(1)
S(1)	1418(2)	3866(2)	4295(2)	52(1)
S(2)	3660(2)	3086(2)	1597(2)	59(1)
N	3874(5)	2614(5)	4994(7)	52(2)
C(1)	1103(8)	6123(6)	2254(9)	56(3)
C(2)	2893(8)	5780(6)	−782(10)	77(3)
C(3)	−59(9)	3066(6)	985(11)	71(3)
C(4)	3079(6)	3146(5)	3692(8)	44(2)
C(5)	3396(8)	2589(6)	6811(8)	64(3)
C(6)	3024(9)	1498(7)	7003(10)	84(4)
C(7)	5298(8)	2024(9)	4650(12)	90(4)
C(8)	6134(10)	2878(11)	5008(13)	139(7)
C(10)	1812(7)	2136(5)	1038(9)	49(3)
C(11)	2931(7)	8385(6)	451(9)	58(3)
C(12)	3134(8)	9469(7)	977(11)	72(4)
C(13)	2248(10)	10304(7)	2066(11)	74(4)
C(14)	1121(10)	10079(7)	2658(12)	86(4)
C(15)	907(8)	8998(6)	2150(11)	73(3)

[a] E.s.d.s are given in parentheses.
[b] Equivalent isotropic U defined as 1/3 of the trace of the orthogonalized U_{ij} tensor.

Table 9
Bond lengths (Å) and angles (°) [a] for $[Au_2(CH_2PPh(Me)CH_2)_2(S_2CN(Et)_2)_2]$

Au–S(1)	2.433(2)	Au–C(1)	2.097(8)
Au–C(3)	2.092(9)	Au–AuA	2.647(1)
P–C(1)	1.731(8)	P–C(2)	1.789(7)
P–C(10)	1.818(7)	P–C(3A)	1.762(9)
S(1)–C(4)	1.737(6)	S(2)–C(4)	1.685(7)
N–C(4)	1.362(8)	N–C(5)	1.470(9)
N–C(7)	1.459(9)	C(3)–PA	1.762(9)
C(5)–C(6)	1.49(1)	C(7)–C(8)	1.52(2)
C(10)–C(11)	1.38(1)	C(10)–C(15)	1.386(9)
C(11)–C(12)	1.39(1)	C(12)–C(13)	1.35(1)
C(13)–C(14)	1.37(1)	C(14)–C(15)	1.39(1)
S(1)–Au–C(1)	89.1(2)	S(1)–Au–C(3)	86.5(2)
C(1)–Au–C(3)	175.2(3)	S(1)–Au–AuA	178.3(1)
C(1)–Au–AuA	91.7(2)	C(3)–Au–AuA	92.6(2)
C(1)–P–C(2)	110.5(3)	C(1)–P–C(10)	112.9(3)
C(2)–P–C(10)	107.3(4)	C(1)–P–C(3A)	106.9(4)
C(2)–P–C(3A)	108.6(4)	C(10)–P–C(3A)	110.6(3)
Au–S(1)–C(4)	101.5(2)	C(4)–N–C(5)	124.0(5)
C(4)–N–C(7)	120.8(6)	C(5)–N–C(7)	115.3(6)
Au–C(1)–P	112.3(3)	Au–C(3)–PA	112.2(4)
S(1)–C(4)–S(2)	121.6(4)	S(1)–C(4)–N	116.3(5)
S(2)–C(4)–N	122.1(4)	N–C(5)–C(6)	112.5(6)
N–C(7)–C(8)	111.4(7)	P–C(10)–C(11)	123.4(4)
P–C(10)–C(15)	118.5(6)	C(11)–C(10)–C(15)	118.0(7)
C(10)–C(11)–C(12)	120.2(6)	C(11)–C(12)–C(13)	121.3(9)
C(12)–C(13)–C(14)	119.5(8)	C(13)–C(14)–C(15)	119.9(7)
C(10)–C(15)–C(14)	121.1(8)		

[a] E.s.d.s are given in parentheses.

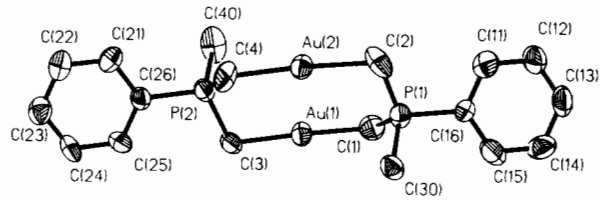

Fig. 1. Thermal ellipsoid drawing (50% probability) of **2**, *trans*-$[Au(CH_2)_2PPhMe]_2$.

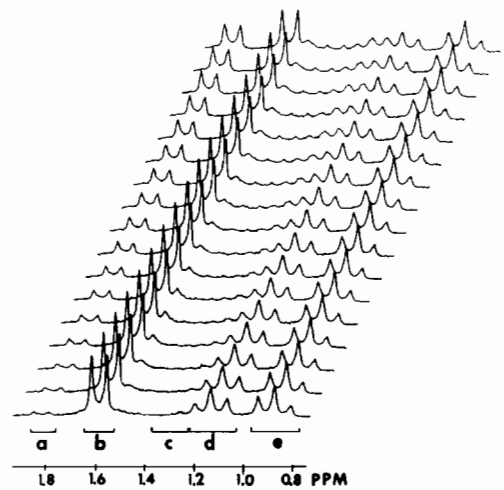

Fig. 2. Change in ^1H NMR spectra of *trans*-**2** with time in a CD_2Cl_2 solution. Spectra taken every 45 min. Region a is the methyl doublet of the *cis* isomer. Region b is the methyl doublet of the *trans* isomer. Region c is one methylene ABX component for the *cis* isomer. Region d is a methylene component for the *trans* isomer. Region e contains the second ABX component for both the *cis* and *trans* isomers of **2**.

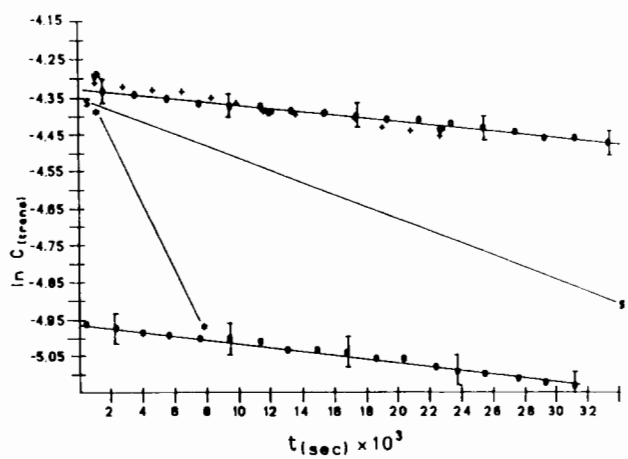

Fig. 3. First-order plots for the rate of disappearance of the *trans* isomer. Plots of the change in concentration of *trans*-**2** with time for various isomerization reactions. Isomerization in the presence of SO_2 is shown by $. Isomerization with added CD_3CO_2D is shown by *.

The disordered structure of **3**, Fig. 5, was solved in the space group $P2_1/c$, which was uniquely defined from its systematic absences. Initially the structure was solved

Table 10
Observed rate constants for the isomerization of **2** in CD_2Cl_2

T (°C)	$[2]\times10^{-5}$ (M)	$k_{obs}\times10^{-6}$	E_a (kJ mol^{-1})
35.0	0.776	4.60	
	1.42	4.63	77.8
30.0	1.39	2.88	
38.5	1.38	6.46	

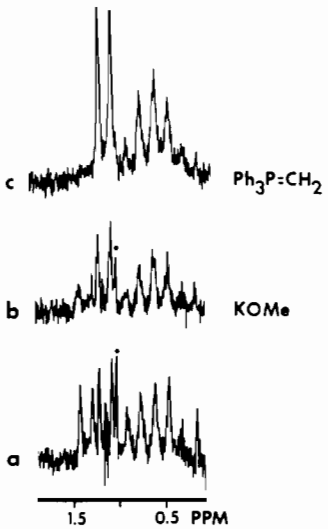

Fig. 4. ^{1}H NMR spectra demonstrating the suppression of isomerization in *trans*-**2** by the addition of base. Plot a is with no added base, plot b is in the presence of $KOCH_3$. Plot c is in the presence of $Ph_3P(CH_2)$. Plots are at 90 MHz, * is impurity peak.

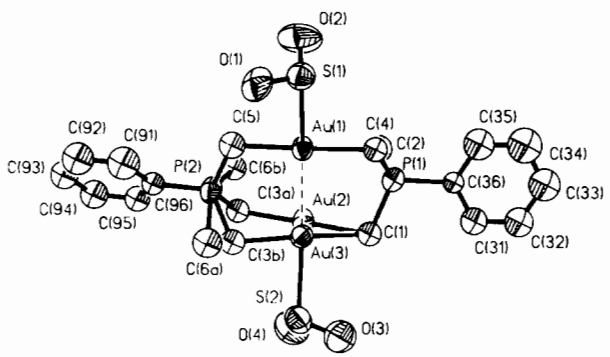

Fig. 5. Molecular structure of **3**, $[Au(CH_2)_2PPhMeSO_2]_2$, showing the disorder due to *cis*/*trans* isomers.

as a simple dimer system ($R=0.091$) but toward the end of refinement a disorder model was added which improved the structure (final $R=0.0540$). This disorder is based on a mixture of the *cis* and *trans* isomers occupying positions in the crystal lattice. The structure contains the *trans* isomer as the dominate isomer (approximately 60%). The solution used to derive the crystal for this crystal structure contained an equilibrium mixture of two isomers, and produced both red needles and small green plates. ^{1}H NMR spectra of the red crystals revealed them to contain approximately 70% *trans* isomer and 30% *cis* isomer. The green crystals showed approximately 70% *cis* isomer and 30% *trans* isomer. A red crystal was used in data collection for the structure of **3**.

The disorder model employed consists of a positional disorder for three atoms, one gold atom (refined as Au(2) and Au(3)), one methylene carbon atom (refined as C(3a) and C(3b)), and one methyl carbon atom (refined as C(6a) and C(6b)). Only one sulfur atom bonded to Au(2) or Au(3), refined as S(2a), can be found in the system (see Fig. 5). The other sulfur atom expected in a disorder caused by the presence of both *cis* and *trans* isomers appears to be absent completely from the data. All of the other atom positions were substantially identical for the two isomers, although one molecule of four (*cis* and *trans*) appears to be absent from the structure. It is the packing of the phenyl rings in the equatorial positions that leads to the observed disorder, since this packing forces the two isomers to assume different geometrical conformations, i.e. the *trans* isomer consists of a chair conformation about the eight-membered gold–ylide ring, while the *cis* isomer must assume the twist-boat conformation to keep its phenyl rings in the equatorial positions. This disorder is limited to one methyl group which is disordered either above (*cis*) or below (*trans*) the plane of the eight-membered ring and to a disorder in one Au atom and the methylene C and sulfur atoms bonded to it. These disorders result from keeping the phenyl ring and the phosphorus atom positions identical in the two conformations while constraining the rest of the molecule to accept either the chair or boat conformations. Most of the atoms in the two conformations can be superimposed and the differences between them alleviated by the disorder observed.

The disorder displayed by **3** complicates a complete analysis of the coordination of SO_2 to this gold dimer. The Au(1)–S(1) portion of the structure is clear, since no disorder is present in this portion of the molecule. The Au(1)–S(1) distance is 2.645(8) Å, a long Au–S interaction. The S(1)–O distances are nearly equivalent, 1.436(20) and 1.411(25) Å. The geometry about S(1) when coordinated to the gold atom is pyramidal. The coordination of the second SO_2 to the dimer unit is less clear due to the disorder of Au. The Au(3)–S(2b) distance is 2.551(11) Å, considerably shorter than the Au(1)–S(1) distance. The Au(2)–S(2a) distance is much longer, however, at 3.01 Å. The S(2)–O distances are equivalent within a standard deviation, averaging 1.423(29) Å. The coordination geometry about the S atom is again pyramidal. The Au–Au distances are 2.894(12) and 2.868(10) Å for Au(1)–Au(2) and Au(1)–Au(3), respectively. The Au–methylene distances range from 2.09(3) Å for Au(2)–C(1) to 2.15(2) Å for Au(1)–C(2). The disordered methylene–Au distances

are within this range. The P–C distances are all normal, except for the short 1.60(5) Å distance for P(2)–C(3a). The C–Au–C angles are nearly linear ranging from 172(2) to 179(1)°. The Au–Au–S angles are not linear.

The structure of **4**, Fig. 6, was solved in the space group *C2/c* with a half molecule in the asymmetric unit. Compound **4** was found to consist of a gold ylide dimer in the chair configuration containing an SO_2 molecule bound to each metal center. The dimer unit has typical P–C bond distances (1.78(1)–1.81(1) Å). The Au–C distances are also normal, 2.10(1) and 2.06(1) Å. The C–Au–C angle is essentially linear (177.8(4)°). The Au–Au distance is 2.835(1) Å. The Au–S distance is 2.587(5) Å with an Au–Au'–S angle of 170.8(1)°. The SO_2 molecule shows a disorder in the position of one oxygen atom (each position refined as 50% occupancy). The S–O distances for S(1)–O(1) of 1.398(15) Å and for S(1)–O(2a) of 1.427(25) Å are nearly identical. The geometry for the sulfur atom using this arrangement is pyramidal. If the arrangement of S(1)–O(1) and S(1)–O(2b) is used, the geometry around S(1) is nearly planar. The S–O distances are also quite different using O(2b) since S(1)–O(2b) is 1.211(31) Å.

The structure of **5**, Fig. 7, is found in the space group $P\bar{1}$ with one half a molecule in the asymmetric cell. As a result of the inversion center, compound **5**

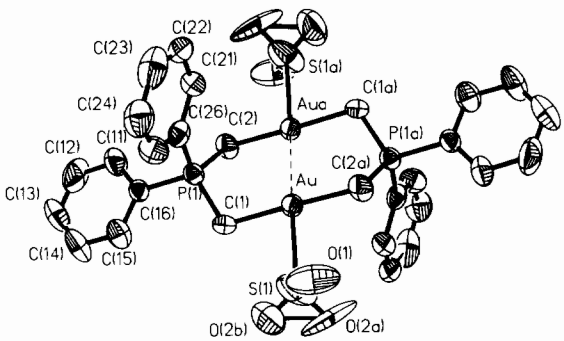

Fig. 6. Molecular structure of **4**, $[Au(CH_2)_2PPh_2SO_2]_2$, with thermal ellipsoids drawn at 50% probability.

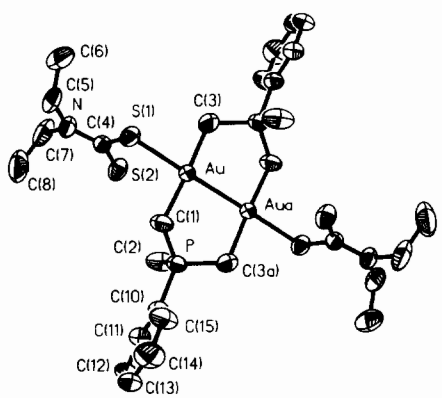

Fig. 7. Molecular structure of **5**, $[Au(CH_2)_2PPhMe]_2[S_2CNEt_2]_2$, with thermal ellipsoids drawn at 50% probability.

has a chair configuration with respect to the eight atoms making up the dimer ring. The structure is the *trans* Au^{II}–Au^{II} isomer. The Au^{II} centers have square planar coordination with a discrete metal–metal bond (2.647(1) Å). The gold–sulfur bond length is 2.433(2) Å and the gold–methylene distances are 2.097(8) and 2.092(9) Å.

4. Discussion

The reaction of Ph_3PAuCl with $Li[(CH_2)_2PMeC_6H_5]$ produces a single isomer of **2** in greater than 90% isomeric purity. The identity of this isomer was subsequently shown to be that of the *trans* isomer by X-ray crystallography. This *trans* isomer will undergo isomerization to an equilibrium mixture of the *cis* (47%) and *trans* (53%) isomers in solution. A kinetic study of this isomerization process was carried out in CD_2Cl_2 by ^1H NMR. Although CH_2Cl_2 is known to react with these dimeric systems under more extreme conditions [13], other solvent systems were ruled out due to the insolubility of **2** or to non-linear kinetic behavior in the early stages of isomerization. No products from the reaction of **2** with solvent were observed over the course of the kinetic studies. Kinetic data showed the isomerization process, Fig. 3, to be first-order in complex **2**, with an activation energy of approximately 83.7 kJ mol^{-1}.

Two studies related to the isomerization of **2** have appeared in the literature of dinuclear gold ylide compounds. Jandik and Schmidbaur [8] demonstrated that ylide ligand exchange occurs by separating a mixed ylide dimer [5] using HPLC from a CH_2Cl_2 solution originally containing only the dimethyl and the di-t-butyl Au(I) ylide dimers, Scheme 1. Secondly, the ring

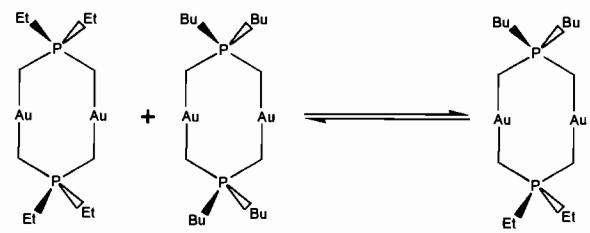

Scheme 1. The exchange of ylide ligands observed in CH_2Cl_2 by Jandik and Schmidbaur using HPLC [8].

cleavage reactions observed in these ylide dimer systems using hydrogen halides [9] suggest a possible mechanism for the isomerization pathway in which the first step would involve the breaking of a single gold–carbon bond to produce a species containing one bridging and one dangling ylide unit. Proton transfer from a methyl carbon to the uncoordinated methylene, followed by rotation and formation of a new Au–CH_2 bond would produce the other isomer. Proton transfer processes such as this are common [14] in ylide systems which contain acidic protons.

While **2** will isomerize from the *trans* isomer to a mixture of *cis* and *trans* isomers in THF and toluene, the isomerization does not occur during the synthesis, presumably because excess ylide anion acts as a strong base which suppresses isomerization. Base suppression was studied by comparing the amount of isomerization of *trans*-**2** in THF with and without the presence of added base. The addition of weak bases showed some suppression and the *isomerization was completely suppressed* by adding the ylide base $Ph_3P(CH_2)$.

Acid catalysis of the isomerization of **2** was observed by comparing the amount of isomerization which occurred when CH_3CO_2H was added to *trans*-**2** with the rate for isomerization without acid, Fig. 3. When two or more equivalents of CF_3CO_2D were added a monomeric cleavage product similar to that observed by Knachel et al. [9] was obtained. If one equivalent of CF_3CO_2D was added, however, only half of **2** was converted to the monomer, with the remainder of **3** quickly isomerizing to the equilibrium mixture of the *cis* and *trans* isomers.

Most mechanisms which account for both the acid catalysis and base suppression involve a proton transfer step. A mechanism for isomerization which includes proton transfer to a methylene center of **2** is expected to show deuterium incorporation into the methyl or methylene centers when deutero-acids are used to catalyze the isomerization. Deuterium incorporation is observed when complete cleavage of the dimer to mononuclear products occurs, but at no time was deuterium incorporation observed in the isomerized dimer products. This result rules out any mechanism which involves proton transfer to the ylide ligand. A mechanism in which Au–C bond rupture occurs and isomerization takes place is viable only as long as there is no step involving proton transfer to the ylide ligand. It also implies that the mechanism proposed for the isomerization process must account for acid catalysis without proton–carbon bond formation.

The increase in the rate of *trans* to *cis–trans* isomerization without D^+ incorporation into the ligand suggests that some process different from H^+ attack at the methylene center is involved in the isomerization. It has been observed that Lewis acids in general cause changes in **2** to occur. While strong Lewis acids form uncharacterized products, weak Lewis acids such as Me_3SnCl, Ph_3PAuCl and SO_2 simply catalyze the isomerization.

While investigating the role of Lewis acids, an SO_2 adduct of **2** was isolated. This complex, **3**, contains SO_2 coordinated to the Au^I centers. Although **3** was investigated by X-ray crystallography, the structure contains a severe disorder attributed to the presence of a mixture of *cis* and *trans* isomers in the lattice. This disorder hindered an accurate evaluation of the bonding at one Au center. At the other Au center, the Au–SO_2 moiety is not complicated by disorder and shows clearly an Au–SO_2 interaction that is pyramidal about the sulfur atom. A pyramidal coordination about SO_2 has been associated with the Lewis acid character of SO_2 [15]. The bond lengths for S(1)–O(1) and S(1)–O(2) are nearly identical, consistent with a formulation approximating an Au^{II} atom coordinated SO_2^-. The coordination is weak, however, and SO_2 can be removed from the solution by pumping. The SO_2 ligand is also lost in the solid state as evidenced by the decomposition of crystalline samples of **3**.

Compound **4** was prepared to confirm the structural features observed in **3**. Since **4** does not have *cis* and *trans* isomers, the major disorder of **3** is eliminated. Compound **4** contains an Au–S interaction with SO_2 bound in the terminal positions. Both **3** and **4** are unique in respect to this feature, and are to the best of our knowledge the first dinuclear species containing SO_2 bound in a terminal position [16]. Other polynuclear SO_2 complexes contain SO_2 bridging the metal centers [15–17]. The structure of **4** clearly shows a long Au–S interaction and a shortened Au–Au distance (2.835 Å). A disorder in **4** also exists, but is limited to a single oxygen on the SO_2 ligand. As a result of this disorder the structure of **4** initially appeared to contain a mixture of planar and pyramidal geometries for SO_2 attached to the gold atoms. However, this is not the case since the sum of the angles about S does not exceed 349° even in the most planar model. In general, planar structures of SO_2 bound to metal centers are considered to involve σ-type interaction with the metal, with SO_2 having a π^* (b_1) orbital available for π backbonding. The planar geometry results from π backbonding into the low lying antibonding orbital of the SO_2 [15,17]. The interaction of the Au centers in **1** and **2** with SO_2 to give pyramidally coordinated SO_2 complexes demonstrates that these dinuclear gold compounds act as nucleophiles with Lewis acids, and that such interactions may be enhanced by the formation of increased Au–Au bonding interactions between the metal atoms.

The SO_2 disorder unfortunately prevents our making a definitive statement about the geometries of *both* SO_2 moieties attached to the same dinuclear gold unit. While one SO_2 clearly is pyramidal and thus functions unequivocally as a Lewis acid, the geometry about the second SO_2 is less clear. For **4**, a nearly planar model for one of the SO_2 units and a pyramidal geometry for the other on the same dinuclear unit but with both units disordered as described cannot be discounted for this centrosymmetric (by crystallographic symmetry) molecule. For **3** the possibility that the geometry about the disordered end of the molecule includes a nearly planar SO_2 unit cannot be ruled out crystallographically.

The unsymmetrical structure observed recently [2] for a $[AuL_3]^+$ adduct to a dinuclear gold(I) anion gives some credence to the suggestion that the bonding of the two SO_2 units to the dinuclear ylide dimer also is not symmetrical.

The coordination of SO_2 in **3** and **4** combined with the increased rate of isomerization of *trans*-**2** when SO_2 is added suggests that the ylide ligand isomerization process is activated by Lewis acids through coordination to the metal centers. This observation is consistent with the rate increase observed when CD_3CO_2D is added to *trans*-**2**, but with no deuterium incorporation into the dimer (vida infra). It suggests that the gold atoms behave as Brønsted bases to proton sources.

A plausible mechanism for the isomerization process, one which accounts for observations made, is shown in Scheme 2. Activation of the gold centers by a Lewis acid, which can include another molecule of the complex through intermolecular auriophilic Au···Au interactions, or to a lesser extent the solvent, is accompanied by an increased intramolecular Au···Au bonding interaction. This allows Au–C bond rupture which can lead to the formation of a chelating ylide ligand at one Au center. Precedent exists for both three- and four-coordinate gold centers containing chelating ylides [19,20]. A symmetrical chelating ylide at one gold center allows either Au–methylene bond to rupture with equal probability. Hence reformation of the dimer occurs as either the *cis* or the *trans* isomer. The formation of a weak Au–Au bond of about 40 kJ mol^{-1} during the Au–C bond breaking process is consistent with an activation energy of approximately 80 kJ mol^{-1} for the isomerization. A homolytic Au–C bond rupture process for the ylide ligand is estimated to have an energy requirement minimum of about 120 kJ mol^{-1}. It should be stressed that while Scheme 2 appears to suggest a intramolecular process for the isomerization, that is not what is implied. The species Y can either be an added acid or another molecule of the complex. The work of Jandik and Schmidbaur [8] dictates that intermolecular rearrangement processes do occur. Indeed, intramolecular rearrangement would not be inhibited by adding excess ylide as observed but base adduct formation (as opposed to acid adduct formation) could inhibit Au···Au interactions.

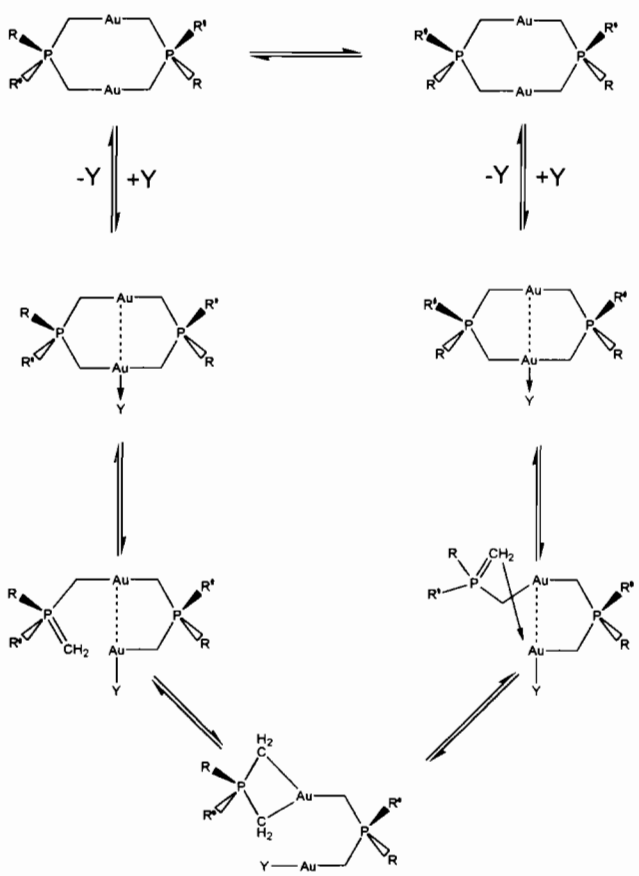

Scheme 2. A scheme representing the proposed mechanism for the isomerization of *trans*-**2**. Y may be either a Lewis acid including another molecule of the complex or the solvent.

This postulated isomerization mechanism implies that when CH_3CO_2H is used to speed up the isomerization process, an Au–H^+ interaction occurs. Although an Au–H interaction has not been proved, the addition of Ph_3PAuNO_3 to *trans*-**2** also catalyzes the isomerization. The formation of the new Au^I product as suggested in the ^1H NMR spectrum, presumably an $AuPPh_3$ adduct, suggests that such acid Au–H interactions are occurring [18]. This mechanism also accounts for the products observed in the ring cleavage reactions with hydrogen halides. Initial interaction of the gold center and opening up of the ring would proceed as described [9]. The presence of a strongly binding anion in solution would compete with the methylene center for the coordination site on Au inhibiting reformation of the dimer ring. Since H^+ has weak coordination at best to Au^I, protonation of the free methylene follows. A second cycle would be required at the second metal center to produce the observed monomeric products [9].

The oxidative addition of **1** has been known to form Au^{II}–Au^{II} metal–metal bonds [4]. The oxidative addition of **2** using Br_2 and Cl_2 has also resulted in the formation of the Au^{II} metal–metal bonded complex [21]. The isomer observed in the crystal structures of these compounds so far has been *trans*. The oxidation of **2** with tetraethyldithiuram disulfide forms the *trans* metal–metal bonded complex.

5. Conclusions

The isomerization process which takes *trans*-$[Au(CH_2)_2PPhMe]_2$ to the equilibrium mixture of *cis*

[2] A crystal structure has been obtained recently for the adduct of $[AuL_3]^+$ to Au^I centers of $[Au_2(i\text{-}MNT)_2]^{2-}$ [18].

and *trans* isomers is acid catalyzed and base suppressed. The catalysis is not due to proton attack at a methylene center but due to nucleophilic attack by the Au atoms of the dimer on the Lewis and/or Brønsted acid centers present in the system. The structures of the SO_2 adducts **3** and **4** determine this Au^I atom basicity through observation of the pyramidal geometry about the S atom of the coordinated SO_2. These SO_2 compounds are the first examples of SO_2 terminally coordinated to a polynuclear metal system.

6. Supplementary material

Lists of structure factors, anisotropic thermal parameters, and hydrogen atom positions (72 pages) are available from author J.P.F.

Acknowledgements

These studies were supported by the National Science Foundation, Grant CHE-9300107, the donors of the Petroleum Research Foundation as administered by the American Chemical Society, and the Welch Foundation.

References

[1] (a) H. Schmidbaur, *Interdiscip. Sci. Rev., 17* (1992) 213; (b) *Gold Bull., 23* (1990) 11; (c) D.M.P. Mingos, *Gold Bull., 14* (1984) 5; (d) R. Uson and A. Laguna, *Coord. Chem. Rev., 70* (1986) 1.

[2] (a) M. Melnik and R.V. Parish, *Coord. Chem. Rev., 70* (1986) 157; (b) R.V. Parish, *Interdiscip. Sci. Rev., 17* (1992) 221.

[3] A.J. Welch and S.K. Chapman (eds.), *The Chemistry of the Copper and Zinc Triads,* Royal Society of Chemistry, Cambridge, UK, 1993.

[4] (a) J.P. Basil, H.H. Murray, J.P. Fackler, Jr., J. Tocher, A.M. Mazany, B. Trzcinska-Bancroft, H. Knachel, D. Dudis, T.J. Delord and D.O. Marler, *J. Am. Chem. Soc., 107* (1985) 6908; (b) H.H. Murray, J.P. Fackler, Jr., L.C. Porter and A.M. Mazany, *J. Chem. Soc., Chem. Commun.,* (1986) 321; (c) H.H. Murray, A.M. Mazany and J.P. Fackler, Jr., *Organometallics, 4* (1985) 154; (d) R.M. Davila, A. Elduque, T. Grant, R.J. Staples and J.P. Fackler, Jr., *Inorg. Chem.,, 32* (1993) 1749; (e) J. Stein, J.P. Fackler, Jr., C. Paparizos and H.-W. Chen, *J. Am. Chem. Soc., 103* (1981) 2192.

[5] (a) H.H. Murray, D.A.Briggs, G. Garzon, R.G. Raptis, L.C. Porter and J.P. Fackler, Jr., *Organometallics, 6* (1987) 1992; (b) R.G. Raptis and J.P. Fackler, Jr., *Inorg. Chem., 29* (1990) 5003.

[6] (a) M.N.I. Khan, J.P. Fackler, Jr., C. King, J.C. Wang and S. Wang, *Inorg. Chem., 27* (1988) 1672; (b) M.N.I. Khan, S. Wang, D.D. Heinrich and J.P. Fackler, Jr., *Acta Crystallogr., Sect. C, 44* (1988) 822; (c) M.N.I. Khan, S. Wang and J.P. Fackler, Jr., *Inorg. Chem., 28* (1989) 3779.

[7] (a) R.G. Raptis, H.H. Murray, R.J. Staples, L.C. Porter and J.P. Fackler, *Inorg. Chem., 32* (1993) 5576; (b) J.D. Basil, *Ph.D. Thesis*, Case Western Reserve University, 1983.

[8] P. Jandik and H. Schmidbaur, *J. Chromatogr., 213* (1981) 47.

[9] H.C. Knachel, C.A. Dettorre, H.J. Galuska, T.A. Salupo, J.P. Fackler, Jr. and H.H. Murray, *Inorg. Chim. Acta, 126* (1984) 7.

[10] C. King, D.D. Heinrich, G. Garzon, J.-C. Wang and J.P. Fackler, Jr., *J. Am. Chem. Soc., 111* (1989) 2300.

[11] B.J. Gregory and C.K. Ingold, *J. Chem. Soc. B,* (1969) 276.

[12] H. Schmidbaur and R. Franke, *Inorg. Chim. Acta, 13* (1975) 85.

[13] P. Jandik, V. Schubert and H. Schmidbaur, *Angew. Chem., 94* (1982) 74; *Angew. Chem., Int. Ed. Engl., 32* (1982) 73; *Angew. Chem., Suppl.,* (1982) 1.

[14] H. Schmidbaur, R. Pichl and G. Muller, *Angew. Chem., Int. Ed. Engl., 25* (1986) 574–575.

[15] R.R. Ryan, G.J. Kubas, D.C. Moody and P.G. Eller, *Struct. Bonding (Berlin), 46* (1981) 47.

[16] (a) M. Cowie and S.K. Dwight, *Inorg. Chem., 19* (1980) 209; (b) A. Wojcicki, *Acc. Chem. Res., 4* (1971) 344; (c) R.R. Ryan and P.G. Eller, *Inorg. Chem., 15* (1976) 494; (d) W.A. Schenk, *Angew. Chem., Int. Ed. Engl., 26* (1987) 98.

[17] D.M.P. Mingos, *Transition Met. Chem. (Weinheim), 3* (1978) 1.

[18] Z. Assefa, R.J. Staples and J.P. Fackler, Jr., *J. Chem. Soc., Chem. Commun.,* (1994) 431.

[19] J.P. Fackler, Jr. and B. Trzcinska-Bancroft, *Organometallics, 4* (1984) 1891.

[20] H.H. Murray, G. Garzon, R.G. Raptis, A.M. Mazany, L.C. Porter and J.P. Fackler, Jr., *Inorg. Chem., 27* (1988) 836.

[21] D.D. Heinrich, *Ph.D. Thesis,* Texas A&M University, College Station, TX, USA, 1987.